APPLICATION OF BACKFACE STRAIN MONITORING TECHNIQUE TO DELAMINATION TEST

J. Jumel[1*], M.K. Budzik[1], N. Ben Salem[1], M. Shanahan[1], P.L. Blanca[2]

[1]*Univ. Bordeaux, I2M, UMR 5295, 351 cours de la libération, F-33400 Talence, France*
[2]*Univ. Bordeaux, CR-IMA, zone aero-portuaire, Rue Marcel Issartier, 33700, Mérignac, France*
**julien.jumel@u-bordeaux1.fr*

Keywords: DCB test, backface strain, cohesive forces, energy release rate

Abstract (Times New Roman 12 pt, bold, single-line spacing, left-aligned text)
DCB test is a popular method for measuring interfaces toughness but also for indentifying cohesive zone models. However, since the measured quantities are global, the test results generally show poor sensitivity to the local cohesive law shape. To improve the test protocol we use backface strain measuring technique to monitor the cohesive forces along the interface facing the crack. A test protocol and data reduction method is proposed based on simple beam on elastic foundation model. From the additional strain measurement, crack position is precisely determined, so as the extension of the cohesive zone. Experimental crack propagation results are presented in case of Mode I delamination test, but also in case of mode I fracture test on CFRP bonded joints.

1 Introduction

Cohesive zone models are now very popular for modeling delamination under complex loading in composite materials [1,2,3,4]. If most of the numerical implementation problems have been solved, these modeling techniques still suffer from a lack of experimental technique to allow proper measurement of cohesive laws. Three main methods prevail. The first one consist in inverse identification from macroscopic data measured during a delamination test using data fitting algorithm [4]. It generally shows poor sensitivity to the cohesive law shape. The second consists in direct measurement on bulk sample using for example Arcan test fixture [5]. Unfortunately, do to the high specimen stiffness it is not possible to accede the softening domain of the cohesive law. The last one is a J integral based approach, which combine local measurement of crack tip relative displacement and macroscopic measurement of J [6]. In this case, since signal derivation is required results sometime appear noisy, but most of all this method requires the assumption of integral J formalism to be verified. To determine a cohesive law, one requires information about relative displacement of the interface but also about the local cohesive forces which are the only missing data. With the backface strain monitoring technique, we use the specimen itself as a load cell to evaluate the local cohesive forces. This method was mainly used to investigate the behavior of adhesively bonded joint using various experimental arrangements [7,8]. It this paper, we apply this technique to monitor the crack propagation and to investigate the process zone in delamination and debonding test on CFRP specimens. The method is based on the use

of effective crack length concept as proposed in [9] so as on the use of beam on elastic foundation model [10]. This method should be improve in near future by combining with direct J evaluation as proposed by [6,11].

2 Materials and testing methods

2.1 Materials and preparation

The DCB specimens are cut from flat plate made with eight plies of Hewply NC-HR 913/35%/132/HTA7 with $[0/-30/30/0]_s$ lay-ups. This laminate was manufactured at CR-IMA using hand lay-up and vacuum bag curing process (1 hour, 125°C). A polypropylene thin film was inserted at the mid-plane of the panel during lay-up to facilitate the initiation of delamination. Natural crack is produced by forcing a thick wedge in between the two arms of the DCB specimen thus producing a ≈40mm natural crack. Hinge load tabs were screwed on aluminum plates which are bonded to the plate with EA9395 toughen epoxy resin adhesive. The specimen is 21 mm large and 150 mm long. After the first delamination test, a CFRP adhesively bonded specimen is fabricated by joining together the two separated arms with SW2216 epoxy paste. The resin and hardener are hand mixed with spatulas. Then a thin layer of adhesive is deposit on both adherends which are press together with spring clips. Reticulation is done in ambient temperature during a day, then the adhesive is postcured at 66°C during one hour. The flexural rigidity of the laminate is calculated with bending test. We find EI_b=0.270N.m^2.

2.2 Instrumented fracture test

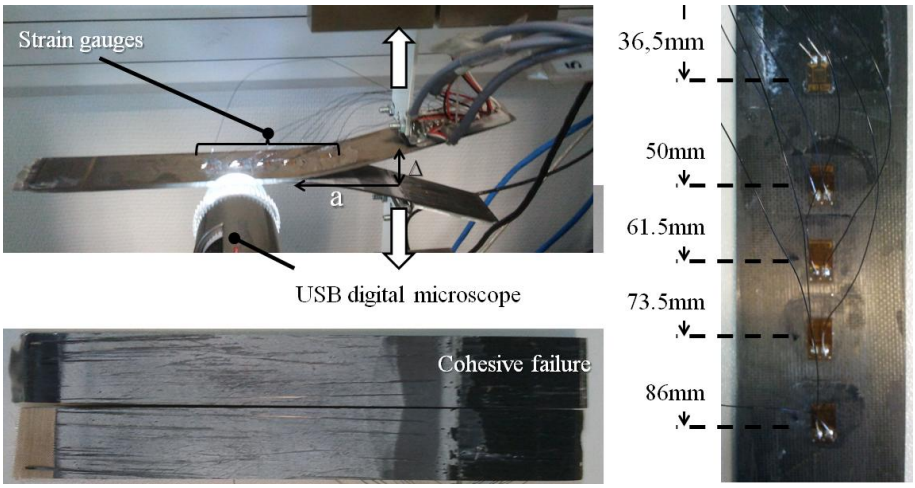

Figure 1. Description of the instrumented DCB test.

The DCB specimens are loaded under constant separation rate using a universal tensile testing machine (Zwick&Roell 010, Zwick Gmbh & Co, Ulm, Germany), instrumented with a 10kN load cell (Zwick&Roell, KAF-TC). The test specimens are instrumented with unidirectional strain gauges (Vishay Micro-Measurements, reference EA-13-060LZ-120/E, nominal resistance 120Ω, grid size 1.5mm) bonded along the midline of the upper side of the plate in the longitudinal direction. Position of the strain gauges with respect to the hinge position are given respectively : specimen 1 : 40mm ; 46mm ; 71mm ; 86mm 101mm ; specimen 2 : 36,5mm ; 50mm ; 61.5mm ; 73.5mm ; 86mm.

A Dino-lite pro camera is used to observe the side of the specimen and monitor the crack propagation and observe directly the damage progress in the cohesive zone. 1280x1024 pixels gray scale images are acquired every five seconds.

3 Backface strain monitoring of DCB test

In the present experiment linear elastic fracture mechanics is applicable. The energy release rate *G* is derived from specimen compliance measurement :

$$C = \frac{\Delta}{F} = \frac{2a^3}{3EI_b} \tag{1}$$

where *a* is the crack length and EI_b is the flexural rigidity of the flexible beam. From relation (1) the classical relation used for evaluating the fracture energy is found :

$$G = \frac{F^2 a^2}{bEI_b} \tag{2}$$

where *b* is the specimen width. From force and displacement measurements and according to relation (1) the instantaneous crack position is evaluated with relation :

$$a = \sqrt[3]{\frac{3EI_b}{2}\frac{\Delta}{F}} \tag{3}$$

Assuming the interface fracture energy is constant during the propagation, the force versus displacement evolution during the crack propagation period is given by relation :

$$F = \sqrt[4]{\left(\frac{8b^3}{9}\right)\left(\frac{2}{EI_b}\right)^5 G_I^{c\,3/4}}\,\frac{1}{\sqrt{\Delta}} \tag{4}$$

which enables simple evaluation of G_I^C. When performing delamination tests on thin laminates, large displacements are sometime observed. The horizontal displacement of the bonded part of the specimen is given by relation :

$$\delta_x = a - \sqrt{\frac{2EI_b}{F}}\sqrt{\sin\theta_0} \tag{5}$$

And the vertical deflection by relation :

$$\Delta = \sqrt{\frac{2EI_b}{F}}\int_0^{\theta_0} \frac{\sin u\,du}{\sqrt{\sin\theta_0 - \sin u}} \tag{6}$$

With θ_0 is the beam rotation at position where load is applied. The beam rotation is related to the interface fracture energy with relation :

$$G = 2\frac{F}{b}\sin\frac{\theta_0}{2} \tag{7}$$

In the previous analysis, the adherends are modelled as Euler-Bernoulli beams and the interface rigidity is supposed to be infinite. To refine the analysis and describe phenomenologically the development of a process zone in front of the crack front we now utilize a Timoshenko beam on a Winkler elastic foundation model. Along the debonded/delaminated part ($0 < x < a$) of the specimen, the deflection is given by :

$$w = \frac{F}{\kappa G_{xy} S}x + \frac{F}{EI_b}\left(a\frac{x^2}{2} - \frac{x^3}{6}\right) + F\theta x + F\delta \tag{8}$$

where G_{xy} is the laminate in-plane shear coefficient, S is the beam section and κ is the shear correction coefficient. θ is the root rotation and δ is the crack tip opening displacement. Along the bonded/unseparated part ($-\infty<x<0$) the beam deflection is given by relation :

$$w = FA_1\exp(\lambda_1 x) + FB_1\exp(\lambda_2 x) \tag{9}$$

coefficients λ_1 and λ_2 are given by :

$$\lambda_{1,2} = \lambda\sqrt{2\left(\varepsilon \pm \sqrt{\varepsilon^2 - 1}\right)} = \lambda\alpha_{1,2} \tag{10}$$

with :

$$\lambda = \frac{\sqrt{2}}{2}\left(\frac{k}{EI}\right)^{1/4} \tag{11}$$

and :

$$\varepsilon = \frac{\sqrt{kEI}}{2\kappa GS} \tag{12}$$

and additional coefficients are given below :

$$A_1 = \frac{a^3}{4EI_b}\frac{\alpha_1}{(\lambda a)^3}\left\{\frac{4\lambda a - \alpha_2^3 + 4\varepsilon\alpha_2}{\alpha_1^3 - \alpha_2^3 + 4\varepsilon(\alpha_2 - \alpha_1)}\right\} \tag{13}$$

$$B_1 = \frac{a^3}{4EI_b}\frac{\alpha_2}{(\lambda a)^3}\left\{\frac{4\lambda a - \alpha_1^3 + 4\varepsilon\alpha_1}{\alpha_2^3 - \alpha_1^3 + 4\varepsilon(\alpha_1 - \alpha_2)}\right\} \tag{14}$$

$$\delta = \frac{a^3}{4EI_b}\frac{1}{(\lambda a)^3}\left\{\frac{\alpha_1\alpha_2(\alpha_1 + \alpha_2) + 4\lambda a}{\alpha_1^2 + \alpha_2^2 - 4\varepsilon + \alpha_1\alpha_2}\right\} \tag{15}$$

$$\theta = \frac{a^2}{4EI_b}\frac{1}{(\lambda a)^2}\left\{\frac{(\alpha_1^2 - 4\varepsilon)(\alpha_2^2 - 4\varepsilon) + 4\lambda a(\alpha_1 + \alpha_2)}{\alpha_1^2 + \alpha_2^2 - 4\varepsilon + \alpha_1\alpha_2}\right\} \tag{16}$$

With these relations, the beam longitudinal strain can be properly derived. Its evolutions along the bonded and debonded parts are given respectively by relations :

$$\varepsilon = F\frac{t}{2}\left(A_1\left({\lambda_1}^2 + \frac{k}{\kappa GS}\right)\exp(\lambda_1 x) + B_1\left({\lambda_2}^2 + \frac{k}{\kappa GS}\right)\exp(\lambda_2 x)\right) \tag{17}$$

$$\varepsilon = F\frac{t}{2EI}(a-x) \tag{18}$$

Additional, useful quantities such as corrected specimen compliance, energy release rate, and apparent crack length from expression (8) as proposed in [8] in order to take into account the effect of interface compliance in the analysis of the test. These phenomenological description indicates that a process process zone is developing in front of the crack tip which is characterized by two coefficients λ and ε, which depend on the interface tensile rigidity and the beam bending and shear compliance. Coefficient λ^{-1} indicates the extension of the process zone which could be properly measured by monitoring the backface strain evolution during the crack propagation period and using relation (17). The additional formulas presented above enable more advanced data reduction method for proper evaluation of the energy release rate, taking into account large displacement effect which will not be presented in this short paper devoted to the presentation of the data reduction method of backface strain measurements and the new information they provide.

4 Application of data reduction technique DCB tests

4.1 Macroscopic analysis

In figure 2 are represented the force versus displacement evolutions as measured during delamination and debonding test on the CFRP specimen and bonded specimen. Brittle elastic behaviour is observed with a weak non-linearity which is mostly due to large displacement effect as explained below. Are also represented the linear fitting before the crack propagation onset, and the curve predicted with relation (4) during the crack propagation phase and using the G=994 J.m^{-2} for the bonded joint and G=586 J.m^{-2} pour for delamination energy which are in good agreement with the experimental findings.

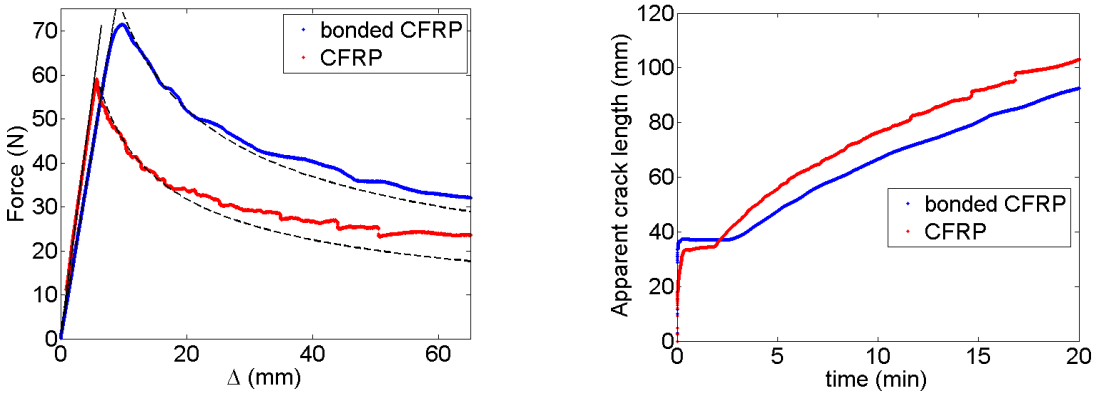

Figure 2. Force versus opening evolution (left) – apparent crack length versus time (right) .

From relation (3) and following the method proposed by [9], we compute the apparent crack length from instantaneous compliance value Δ/F. Crack onset is clearly evidence so as a stable crack propagation regime. This continuous measurement of the apparent crack length

also allow to compute the instantaneous apparent crack speed which shows different types of behaviour as presented in figure 3. Indeed, the crack propagation speed shows large variation in the case of the composite where some instabilities are evidenced, while the propagation is much stable in the case of the bonded joint. After complete separation, the adherend instrumented with strain gauges is loaded in bending to calibrate the strain variation as a function of applied displacement. The beam is tightly fixed on one end with a rigid hinge. On the other end, cyclic constant rate (0.3 mm/min) imposed displacement is applied with increasing step (5mm). Distance between clamping system and applied load is 104 mm. After the maximum displacement is reached, the displacement is maintained during 10s to check for any relaxation phenomenon before unloading which not observed here. The evolution of strain during the holding time as a function of applied displacement is also represented in figure 3. For each gauges the evolution is perfectly linear. From this measurement the "normalized strain" $\varepsilon_i/(\Delta.x_i)$ is found equal to 1.3371 µdef/mm^2. Note that this calibration does not require to measure the material stiffness, but that the fixture that are used in this configuration are slightly different from the one used during the DCB experiment since the clamping system is different.

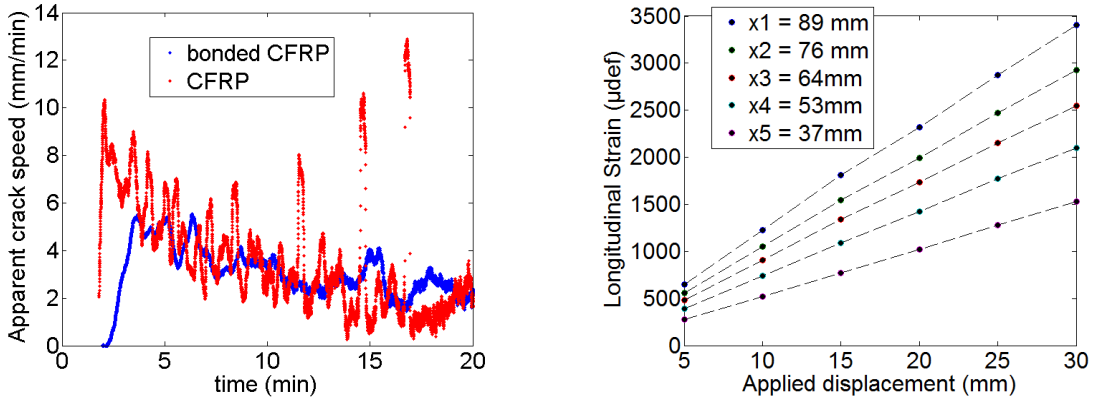

Figure 3. Apparent crack propagation speed versus time (left) – Strain gauges calibration (right) .

4.1 Macroscopic analysis

The time evolutions of strain gauges signal both experiment are presented in figure 4. These evolutions are complexe to interpret, but already enables to detect the vicinity of the process zone when approaching the strain gauges position.

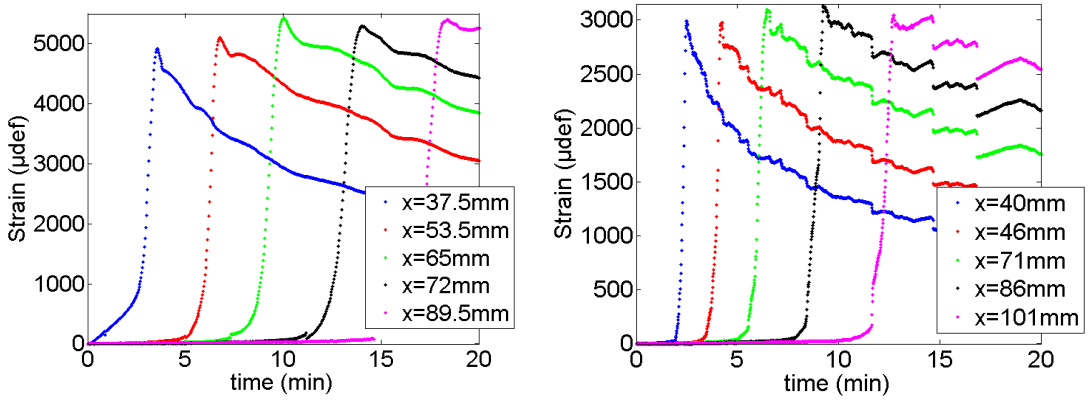

Figure 4. Time evolution of strain gauges signal, bonded joint (left) – delamination test (right)

It should be notice that in this experiment, the sensors (viz. strain gauges) are not scanning the specimen since they are bonded, but that the process zone is monitored anyway since it crosses each strain gauge position.

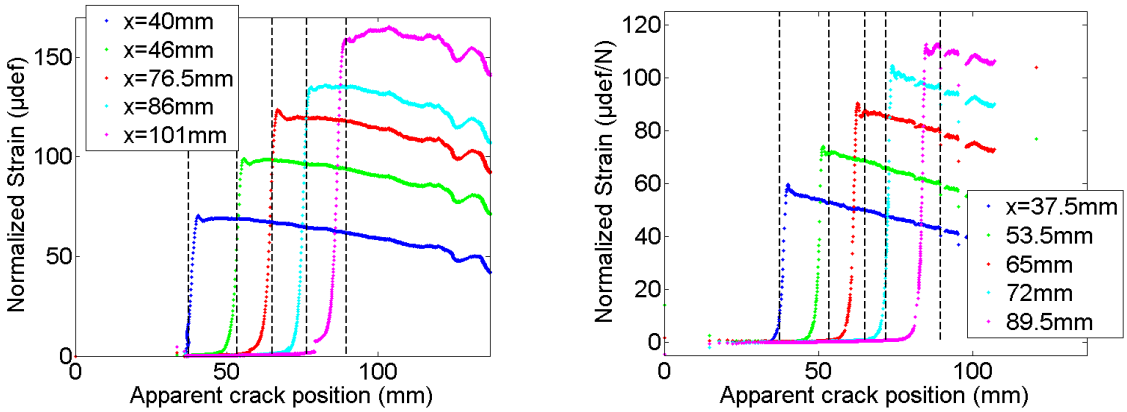

Figure 5. Normalized strain evolution as a function of apparent crack length. Bonded joint (left) – delamination test (right) .

To obtain a strain versus "position" representation which could be compared with the theoretical expressions presented in section 3, the strain measurement are reported as a function of apparent crack position. Since the observed behaviour is macroscopically brittle-elastic, the strain data are normalized (*viz.* divided by the instantaneous applied force). Normalized strain versus apparent crack position evolutions are reported in figure 5. Since the process zone is found to be small in the present experiment, the In figure 5 are reported the force versus opening evolution and the crack length versus time evolution for both the delamination tests and the debonding experiment. The maximum strain is detected when the "crack" is passing under the sensor. Prior maximum strain is reached, the strain is slowly growing over a distance which is much larger than the strain gauges grid size (≈1.5mm). This progressive variation of strain marks the presence of a process zone facing the crack front which is evidence with our technique. In the case of the delamination test the process zone size is ≈7mm while in the case of the bonded joint the process zone size is twice (≈15mm) which indicates a more compliant interface and explains the larger fracture energy that we measure in this case.

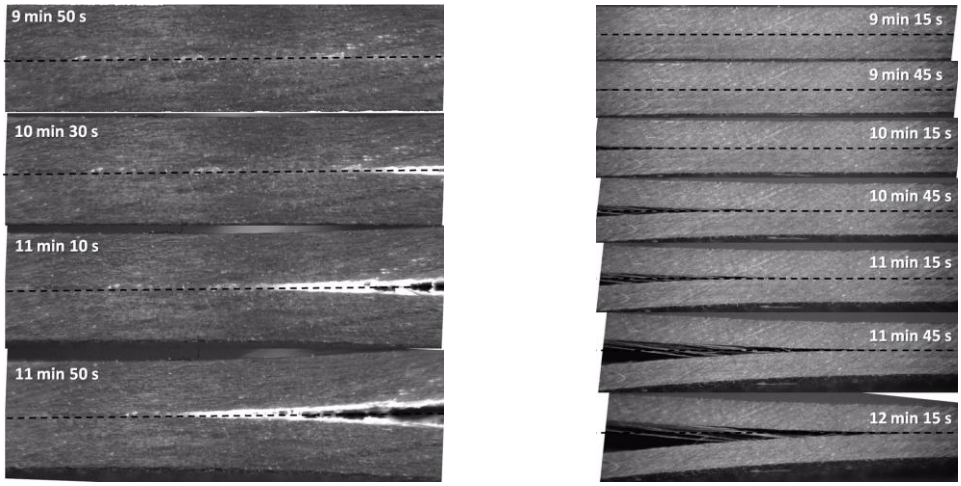

Figure 6. Crack propagation in bonded joint (left) – delamination (right) Adherend thickness is 1 mm

The video monitoring presented in figure 6, confirms this trend. Indeed, a large white cohesive zone is evidenced in the case of the debonding experiment while in the case of the delamination test, very few fiber bridging is observed which does not reinforce the interface. The large process zone observed with this very sensitive technique is also due the stress redistribution in the composite itself due to interlaminar shear. It should also be noticed that the normalized strain is decreasing after the crack has passed the strain gauges position. This phenomenon is attributed to large displacement effect which can be simply quantifies here.

5 Conclusions and perspectives

Backface strain monitoring during DCB test enables direct evaluation of the process zone size in front of the crack and provides additional useful controls of experimental artefact such large displacement effect or irreversible deformation of the adherends. The data reduction method proposed here should be usefull to be combined with other experimental technique for finer investigation of cohesive zone behavior.

References

[1] Robinson P., Das S. Mode I DCB testing of composite laminates reinforced with z-direction pins : a simple model for the investigation of data reduction strategies. *Engineerign fracture mechanics*, **71**, pp. 345-364 (2004).

[2] Högberg J.L., Sorensen B.F., Stigh U. Constitutive behavior of mixed mode loaded adhesive layer. *International journal of solids and structures*, **44**, pp. 8335-8354 (2007).

[3] Borg R., Nilsson L., Simonsson K. Simulating DCB, ENF and MMB experiments using shell elements and a cohesive zone model. *Composites Sciences and Technology*, **64**, pp. 269-278 (2007).

[4] Sun C.T., Jin Z.H. Modeling of composite fracture using cohesive zone and bridging models. *Composites Sciences and Technology*, **66**, pp. 1297-1302 (2006).

[5] Cognard J.Y., Créac'hcadec R., Sohier L., Davies P., Analysis of the nonlinear behavior of adhesives in bonded assemblies—Comparison of TAST and Arcan tests. *International Journal of Adhesion and Adhesives*, 28, pp. 393-404 (2008).

[6] Gunderson J.D., Brueck J.F., Paris A.J., Alternative test method for interlaminar fracture toughness of composites. *International Journal of Fracture*, **143**, pp. 273-276 (2007).

[7] Budzik M., Jumel J., Imielinska K., Shanahan M.E.R. Accurate and continuous adhesive fracture energy determination using an instrumented wedge test. *International Journal of Adhesion & Adhesives*, **29**, pp. 694-701 (2009).

[8] Budzik M., Jumel J., Shanahan M.E.R., Process zone in the single cantilever beam under transverse loading – Part II : Experimental. *Theoretical and Applied Fracture Mechanics*, 56, pp. 12-21 (2011).

[9] De Morais A.B., Pereira A.B. Application of the effective crack method to mode I and mode II interlaminar fracture of carbon/epoxy unidirectional laminates. *Composites: Part A*, **38**, pp. 785-794 (2007).

[10] Shokrieh M.M., Heidari-Rarani M., Ayatollahi M.R. Calculation of G_I for a multidirectional composite double cantilever beam on two-parametric elastic foundation. *Aerospace Science and Technology*, **15**, pp. 534-543 (2011).

[11] Ji G., Ouyang Z., Li G., On the interfacial constitutive laws of mixed mode fracture with various adhesive thickness. *Mechanics of Materials*, **47**, pp. 24-32 (2012).